[CANCER RESEARCH 62, 5308–5316, September 15, 2002]

# Dissecting the Oncogenic Potential of Gli2: Deletion of an $NH_2$-Terminal Fragment Alters Skin Tumor Phenotype[1]

**Hong Sheng, Sara Goich, Aiqin Wang, Marina Grachtchouk, Lori Lowe, Rong Mo, Kui Lin, Frederic J. de Sauvage, Hiroshi Sasaki, Chi-chung Hui, and Andrzej A. Dlugosz[2]**

*Comprehensive Cancer Center and Departments of Dermatology [H. Sh., S. G., A. W., M. G., L. L., A. A. D.] and Pathology [L. L.], University of Michigan, Ann Arbor, Michigan 48109; Program in Developmental Biology, Hospital for Sick Children, and Department of Molecular and Medical Genetics, University of Toronto, Toronto, Ontario M5G 1X8, Canada [R. M., C-c. H.]; Department of Molecular Oncology, Genentech, South San Francisco, California 94080 [K. L., F. J. d. S.]; and Laboratory of Developmental Biology, Institute for Molecular and Cellular Biology, Osaka University, Osaka 569-0871, Japan [H. Sa.]*

## ABSTRACT

**Development of basal cell carcinomas (BCCs) in skin is associated with uncontrolled Sonic hedgehog (Shh) signaling, which operates primarily through the Gli family of transcription factors. Gli2 is a mediator of physiological Shh signaling in skin and is sufficient to produce BCCs when overexpressed by use of a *Keratin 5* (*K5*) promoter. Analysis of Gli protein deletion mutants has identified an $NH_2$-terminal transcription repressor domain in Gli2 but not Gli1. To assess the potential involvement of the Gli2 repressor domain in skin tumor development, we overexpressed the Gli2ΔN2 mutant in transgenic mice by use of the *K5* promoter. *K5-Gli2ΔN2* mice developed a variety of skin tumors resembling human trichoblastomas, cylindromas, basaloid follicular hamartomas, and rarely, BCCs. In striking contrast, *K5-Gli2* mice overexpressing wild-type Gli2 developed only BCCs. Other differences between tumors arising in these two sets of transgenic mice included their gross appearance, growth rate, and predilection for specific body sites. However, the expression levels of Shh target genes, which reflect the magnitude of Shh pathway activation, were not dramatically different. Tumors from *K5-Gli2ΔN2* mice, unlike human or mouse BCCs, gave rise to cell lines that constitutively expressed Shh target genes *in vitro* and were tumorigenic in nude mice. Interestingly, the phenotype of *K5-Gli2ΔN2* mice was strikingly similar to that reported after *K5* promoter-driven overexpression of GLI1, which lacks an $NH_2$-terminal region homologous to the Gli2 repressor domain. These results underscore the qualitative difference in oncogenicity of GLI1 and Gli2 when overexpressed in skin, and reveal a previously unanticipated role for the Gli2 $NH_2$ terminus in defining tumor phenotype.**

## INTRODUCTION

Shh[3] regulates patterning and growth of a remarkable variety of tissues throughout embryogenesis (reviewed in Refs. 1, 2). Shh binds and reversibly inhibits the cell-surface receptor Ptch, which antagonizes the action of Smoothened (reviewed in Refs. 2, 3). Shh-mediated derepression of Smoothened results in up-regulation of Shh target genes, including *Ptch1* and *Gli1*. Studies in *Drosophila* indicate that hedgehog modulates gene expression through the zinc finger-containing transcription factor Ci, which can function as either a transcriptional activator or proteolytically cleaved repressor (reviewed in Ref. 4). In vertebrates, transcriptional responses to Shh and other hedgehog proteins are mediated by the three Ci homologues Gli1, Gli2, and Gli3 (reviewed in Refs. 2, 5, 6), which work in concert to modulate target gene expression. Gli1 and Gli2 appear to act primarily as transcriptional activators, whereas Gli3 functions largely as a repressor.

Although *Gli1* mRNA is consistently up-regulated in target cells responding to Shh and in certain settings *Gli1* can mimic responses to Shh (7–9), mice harboring functionally null *Gli1* alleles are born without detectable abnormalities and are viable and fertile (10). In contrast, disruption of *Gli2* function results in developmental defects involving multiple Shh target tissues (11–15), strongly suggesting an obligatory role for Gli2 as a primary effector of Shh signaling. Hair follicle morphogenesis is severely impaired in *Shh* (16–18) and *Gli2*[4] mutants, but not in *Gli1* or *Gli3* mutants. These findings strongly suggest that the physiological effector mediating responses to Shh in normal skin is Gli2.

Although precise spatial and temporal activation of Shh signaling is required during normal embryogenesis, constitutive activation of this pathway is associated with cancer development. Patients with nevoid basal cell carcinoma syndrome exhibit a variety of developmental abnormalities and have a markedly increased incidence of BCCs and several other neoplasms (reviewed in Ref. 19). These individuals harbor germline *PTCH1* mutations and have lost the remaining normal *PTCH1* allele in BCCs (20, 21), resulting in derepression of SMO and hence constitutive SHH pathway activation. *PTCH1* mutations have also been found in >50% of sporadic BCCs (20–24), and SHH target genes *GLI1* and *PTCH1* are up-regulated in nearly all BCCs examined (22, 25, 26), suggesting that uncontrolled activation of the SHH pathway plays a central role in the development of these tumors.

The consistent up-regulation of Shh target genes in BCCs suggests that heightened activity of Shh transcriptional effectors plays a central role in BCC development. Given the requirement for Gli2 in physiological Shh signaling in embryonic hair follicles, we proposed that Gli2 may also have a crucial function in pathological, constitutive Shh signaling in BCCs. To test this hypothesis, we engineered transgenic mice expressing *Gli2* driven by a *K5* promoter (27). *K5-Gli2* mice spontaneously developed multiple BCCs (28), suggesting an important role for Gli2 in BCC formation triggered by upstream activation of the Shh pathway. Interestingly, overexpression of *GLI1* using the same *K5* transgenic cassette resulted in a distinct phenotype, characterized by the appearance of multiple types of skin tumors, with a minority being BCCs (29).

On the basis of assays measuring transcriptional activity by use of an 8xGli-binding site luciferase reporter, Gli2 was shown to contain an $NH_2$-terminal repressor domain that is not present in Gli1 (30). To test the involvement of the Gli2 $NH_2$ terminus in BCC tumorigenesis, we overexpressed the *Gli2ΔN2* mutant in skin, using the *K5* promoter. Although differing in several respects from *K5-Gli2* mice (28), *K5-Gli2ΔN2* mice resembled transgenic mice in which *GLI1* was driven by the same promoter (29). Our findings strongly implicate the $NH_2$-terminal repressor domain of Gli2 in the distinct tumor phenotypes produced by skin-targeted overexpression of *Gli2 versus GLI1*.

Received 1/9/02; accepted 7/9/02.

The costs of publication of this article were defrayed in part by the payment of page charges. This article must therefore be hereby marked *advertisement* in accordance with 18 U.S.C. Section 1734 solely to indicate this fact.

[1] Supported in part by NIH Grant RO1 CA87837, Cancer Center Support Grant P30 CA046592, Dermatology Training Grant T32 AR07197 (to H. Sheng), and a Terry Fox New Frontiers Award from the National Cancer Institute of Canada (to C-C. H.)

[2] To whom requests for reprints should be addressed, at the Department of Dermatology, 3310 CCGC Box 0932, 1500 E. Medical Center Drive, Ann Arbor, MI 48109-0932. Phone: (734) 647-9482; Fax: (734) 763-4575; E-mail: dlugosza@umich.edu.

[3] The abbreviations used are: Shh, Sonic hedgehog; Ptch, Patched; BCC, basal cell carcinoma; K5, keratin 5.

[4] P. Mill *et al.*, manuscript in preparation.

## MATERIALS AND METHODS

**Transfection and Reporter Assays.** SV40-transformed human keratinocytes (Ref. 31; obtained from Dr. Richard Schlegel, Georgetown University, Washington, DC), were subcultured into 6-well plates at a density of $2 \times 10^5$ cells/well the day before transfection. Cells were cotransfected with reporter plasmid (0.3 $\mu$g) containing eight copies of a 30-bp sequence containing the Gli binding site (GAACACCA) from the mouse *Hnf3β* (*Foxa2*) promoter, a δ-crystalline minimal promoter, and luciferase cDNA (32); control plasmid (SV-β-gal; 0.1 $\mu$g); and effector plasmid (0.6 $\mu$g), either pcDNA3.1HisB (vector control), pcDNA3.1HisBGli2, or pcDNA3.1HisBGli2ΔN2 (30). Transfections were performed with 3 $\mu$l of FuGENE6 reagent (Roche) according to the manufacturer's protocol. Cells were harvested 48 h after transfection, and luciferase levels were determined as described previously (33). β-Galactosidase activity was used to normalize for transfection efficiency.

**Generation and Identification of *K5-Gli2ΔN2* Transgenic Mice.** *Gli2ΔN2* cDNA containing an $NH_2$-terminal His tag was released from pcDNA3.1HisBGli2ΔN2 by digestion with *Bst*98I and *Not*I, subcloned into the *Sna*BI site of the bovine *K5* transgenic cassette kindly provided by Dr. Jose Jorcano (CIEMAT, Madrid, Spain; Ref. 27), and verified by sequencing. The *K5-Gli2ΔN2* transgene was released by use of *Bss*H, purified, and microinjected into (C57BL/6×SJL) F2 mouse eggs by personnel at the University of Michigan Transgenic Core. The same genetic background was used to produce *K5-Gli2* mice (containing a Gli2 $NH_2$-terminal FLAG epitope tag) that we described previously (28), and C57BL/6J×CBA F2 oocytes were used by Toftgard *et al.* (29) to produce *K5-GLI1* mice. Transgenic mice were identified by PCR analysis of tail DNA using vector-specific primer (5′-CCCATATGTCCTTCCGAGTG-3′) and *Gli2ΔN2*-specific primer (5′-ATTCCTTGACACTGCCCTCCATCC-3′). Animals were housed according to University of Michigan institutional guidelines.

**RNA Isolation and Analysis.** RNA from skin and skin tumors was extracted after homogenization in TRIzol reagent (Invitrogen Life Technologies, Inc.). The reverse transcription reaction was performed at 42°C for 50 min with 1 $\mu$g of total RNA and 0.25 $\mu$g of random primers. PCR was performed with *Gli2ΔN2* transgene-specific primers (5′-ACTGGTGGACAGCAAATGGG-3′ and 5′-GAGTTGGGTAGGCATGGTGC-3′) and *β-actin* primers (5′-TACCACAGGCATTGTGATGGA-3′ and 5′-CAACGTCACACTTCATGATGG-3′). For Northern blotting, 10 $\mu$g of each total RNA sample were separated on a 1.2% agarose formaldehyde gel, transferred to Zeta-Probe nylon membrane (Bio-Rad), and hybridized overnight at 42°C to $^{32}$P-labeled cDNA probes (labeled by random priming) in hybridization buffer, as recommended [50% formamide, 0.12 M $Na_2HPO_4$ (pH 7.2), 0.25 M NaCl, 7% SDS, and 1 mM EDTA] by the manufacturer. Probes were as follows: *Ptch1*, 841-bp 5′ *Eco*RI fragment (kindly provided by Dr. Andrew McMahon, Harvard University, Boston, MA); *Gli1*, 3′ PCR product spanning nucleotides 2655–3321; *Gli2*, a 1-kb fragment (34). Blots were washed at a final stringency of 2× SSC/0.1% SDS at 60°C, exposed to phosphorimager screens, and analyzed using a Storm 840 Phosphorimaging System (Molecular Dynamics). Quantitative PCR was performed using real-time TaqMan technology, and products were analyzed on a Model 7700 Sequence Detector (Applied Biosystems). Two PCR primers and a hybridization probe labeled with a reporter dye, 6-carboxyfluorescein, on the 5′ nucleotide and a quenching dye, 6-carboxytetramethylrhodamine, on the 3′ nucleotide were used (sequences provided on request). Fifty-microliter reactions contained 50 ng of total RNA, 12.5 units of murine leukemia virus reverse transcriptase, 1.25 units of AmpliTaq Gold DNA polymerase, 0.2 units of RNase inhibitor, 1× PCR reaction buffer containing 5 mM magnesium chloride, 165 ng (or 500 nM) of each primer, 300 $\mu$M deoxynucleotide triphosphates, and 100 ng (300 nM) of TaqMan probe. $C_t$ values, corresponding to the cycle number at which the fluorescent emission monitored in real-time reaches a threshold of 10 SD above the mean baseline emission, from cycles 3 up to 15 were measured. Cycling parameters were 30 min at 48°C, 10 min at 95°C, and 40 cycles of 15 s at 95°C and 1 min at 60°C.

**Immunoprecipitation and Western Blot Analysis.** Protein extracts were prepared by homogenizing skin or tumor samples in lysis buffer [50 mM Tris (pH 7.5), 1 mM EDTA, 120 mM NaCl, 1% NP40, 10 $\mu$g/ml leupeptin, 10 $\mu$g/ml aprotinin, 0.5 mM phenylmethylsulfonyl fluoride, 10% glycerol] in an Omni-Probe tissue homogenizer. Protein concentration was determined using the Bio-Rad DC protein assay. For immunoprecipitation, 200 $\mu$g of protein extracts were incubated with 10 $\mu$l of rabbit anti-His polyclonal antibody (M-21; Santa Cruz Biotechnology) and 30 $\mu$l (1:1 slurry in lysis buffer) of protein G-agarose beads (Invitrogen Life Technologies) at 4°C overnight with shaking. The proteins were eluted in 30 $\mu$l of 2× SDS loading buffer. For Western blotting, 30 $\mu$g of protein lysate or 30 $\mu$l of protein eluate from immunoprecipitation were separated on 5–7.5% SDS-PAGE gels and transferred to reinforced nitrocellulose membranes (Schleicher & Schuell). The membranes were blocked with 5% nonfat dry milk in PBS, probed with 1:2000 rabbit anti-His antibody (M-21) for 1 h at room temperature, washed, and incubated with horseradish peroxidase-conjugated donkey antirabbit IgG secondary antibody (Jackson Immunoresearch). Immunoreactive proteins were detected by enhanced chemiluminescence (Amersham Corp.).

**Tissue Harvests, Immunostaining, and *in Situ* Hybridization.** Skin samples were fixed overnight in neutral-buffered formalin or Carnoy's fixative (10% glacial acetic acid, 30% chloroform, 60% absolute ethanol), transferred to 70% ethanol, processed, embedded in paraffin, sectioned at 5 $\mu$m, and stained with H&E. For immunohistochemistry, formalin-fixed sections were boiled in 0.01 M citrate buffer (pH 6) for 10 min and reacted with antibodies against mouse K5 (1:2000; Covance) or K17 (1:2000; gift from Dr. Pierre Coulombe, Johns Hopkins University, Baltimore, MD). Sections fixed with Carnoy's fixative were used for mouse K6 (1:1000; Covance) immunostaining. All sections were blocked with 10% normal goat serum for 30 min, incubated with primary antibody diluted in 2 mg/ml BSA for 1 h at room temperature, rinsed in PBS, incubated with biotinylated secondary antibody (1:10,000; Vector) for 30 min, visualized using the Vectastain ABC kit (Vector) and 3,3′-diaminobenzidine as substrate, and counterstained with hematoxylin. For Bcl-2 immunostaining, formalin-fixed sections were treated with 0.01 M citrate buffer (pH 6), blocked with TNK [100 mM Tris (pH 7.6), 500 mM NaCl, 10 mM KCl, 2% BSA, 0.1% Triton X-100, 1.5% normal goat serum] for 1 h, and incubated at 4°C overnight with anti-Bcl-2 (PharMingen) diluted 1:1000 in TNK. The remainder of the immunostaining protocol was the same as described above. *In situ* hybridization was performed on frozen sections, using digoxigenin-labeled probes as described previously (15). The *Gli2* probe detects both endogenous *Gli2* and *Gli2ΔN2* mRNA produced by the transgene.

**Generation of Established Cell Lines and Tumorigenesis Assays.** Portions of tumors were removed from sacrificed animals and were washed twice with medium (HiCa/10× pen-strep) prepared using modified S-MEM (Invitrogen Life Technologies), 8% FCS (Gemini Bioproducts), penicillin (200 units/ml), streptomycin (200 $\mu$g/ml), and 1.4 mM $CaCl_2$. Tumors were minced and digested using 0.35% type I collagenase (Worthington Biochemical Corporation) in DMEM containing 5% FCS, 200 units/ml penicillin, and 200 $\mu$g/ml streptomycin for 2 h at 37°C with occasional agitation. The remaining clumps of epithelial cells were further disrupted by triturating with a 10-ml pipette, washed twice with HiCa/10× pen-strep medium, and plated in type I collagen-coated tissue culture wells in modified S-MEM containing 8% FCS (Gemini Bioproducts), penicillin (20 units/ml), streptomycin (20 $\mu$g/ml), 1.4 mM $CaCl_2$, and 1 ng/ml keratinocyte growth factor (R&D Systems). After 24–36 h, the cells were switched to Lo/K/C medium [S-MEM, 8% $Ca^{2+}$-depleted FCS (35), 0.05 mM $CaCl_2$, 1 ng/ml keratinocyte growth factor, 50 ng/ml cholera toxin (Calbiochem), 20 units/ml penicillin, and 20 $\mu$g/ml streptomycin] and fed every 2–3 days. Cells were subcultured periodically until homogeneous, robust cell lines emerged. Spontaneously immortalized control cell lines were established from *Gtrosa26* (36) mouse skin keratinocyte cultures (35) that were grown in Lo/K/C for several weeks, during which the majority of cells underwent crisis. After allowing for expansion of the surviving cells in the original dishes, cultures were passaged repeatedly until homogeneous cell lines were established. To test for tumorigenicity, cell lines grown in T-175 flasks were trypsinized and injected s.c. ($5 \times 10^6$ cells in 100 $\mu$l of HiCa medium) into 10–11-week-old nude mice (*nu/nu-nu*BR; Charles River), which were examined once or twice per week and harvested 25 days after injection.

## RESULTS

**Increased Activity of *Gli2ΔN2* Deletion Mutant in Cultured Keratinocytes and Skin-targeted Overexpression in Transgenic Mice.** Full-length mouse Gli2 is a relatively weak transcriptional activator in rat neural MNS70 cells, and removal of the $NH_2$-terminal 279 amino acids to produce the Gli2ΔN2 mutant enhances transcriptional activity up to 15-fold (30). We obtained similar results with

cultured keratinocytes: Gli reporter activity was up to 10-fold higher in cells transfected with *Gli2ΔN2* than wild-type *Gli2* expression vector (Fig. 1*A*). These findings support the concept that the $NH_2$ terminus of Gli2 contains a domain that acts as a transcriptional repressor in a variety of cultured cell types.

We have previously shown that overexpression of full-length Gli2 in skin by use of a transgene containing the bovine *K5* promoter (*K5-Gli2*) results in the exclusive appearance of BCCs (28). To examine the role of the Gli2 repressor domain in BCC biology, we overexpressed Gli2ΔN2 in mouse skin, using the same *K5* transgenic cassette (Fig. 1*B*). The *K5* promoter was selected because it is active in the epidermal basal layer and outer root sheath of hair follicles, which contains stem cells (37) that are believed to be tumor precursors (38). Eighteen transgenic founders were identified by PCR-based genotyping, and 5 of these developed multiple skin tumors. We verified transgene expression by reverse transcription-PCR using RNA from skin of several founders exhibiting a skin phenotype (Fig. 1*C*). Using an antibody against the His epitope tag in immunoblots, we detected exogenous Gli2ΔN2 protein with the expected molecular weight in lysates obtained from tumors but not normal-appearing skin (Fig. 1*D*). In an effort to increase sensitivity, we also immunoprecipitated cell lysates that were then examined by immunoblotting. Although this resulted in a stronger band from tumor lysates, Gli2ΔN2 protein was still not clearly detected in normal skin of transgenic mice. These findings suggest that tumors can develop only when cells express a sufficiently high level of Gli2ΔN2.

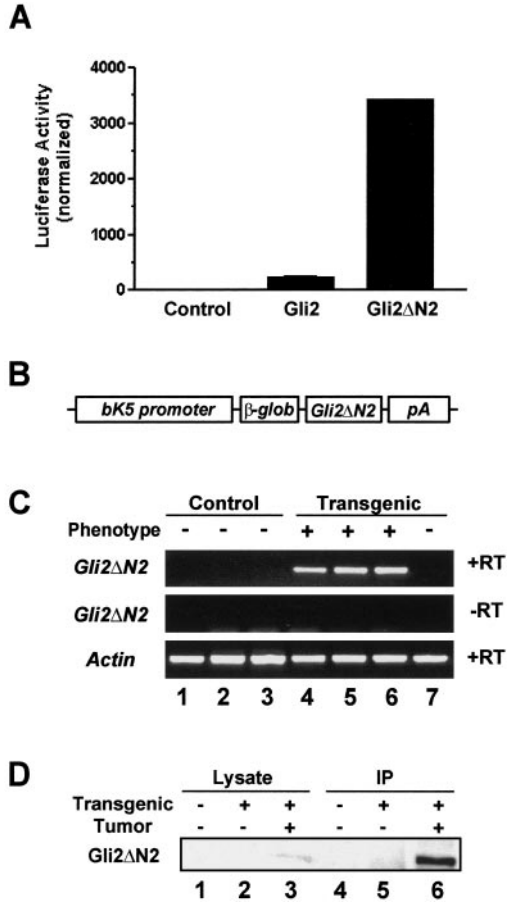


Fig. 1. Heightened transcriptional activity of Gli2ΔN2 *in vitro*, transgene design, and confirmation of *Gli2ΔN2* expression *in vivo*. *A*, Gli2 contains an $NH_2$-terminal repressor domain. Reporter assays were performed in keratinocytes transfected with an 8xGli binding-site luciferase reporter and empty vector (*Control*), effector plasmid with full-length Gli2 (*Gli2*), or an $NH_2$-terminal Gli2 deletion mutant (*Gli2ΔN2*). Cotransfection with a *lacZ* expression plasmid was used to normalize transfection efficiency, and cell lysates were prepared 48 h after transfection. *Columns* represent mean values from two independent dishes, with the range indicated by *error bars*. *B*, transgenic construct containing 5.3-kb bovine *K5* promoter, rabbit *β-globin* intron, $NH_2$-terminal His-tagged mouse *Gli2ΔN2* cDNA, and composite rabbit *β-globin/SV40* poly(A) sequence. *C*, reverse transcription-PCR performed using RNA from three control (*Lanes 1–3*) and four transgenic (*Lanes 4–7*) mouse skin samples using transgene-specific and *β-actin* primers. Note absence of detectable transgene expression in sample from transgenic mouse without a visible phenotype (*Lane 7*). *RT*, reverse transcriptase. *D*, anti-His tag immunoblot of lysates and immunoprecipitations (*IP*) performed with control mouse skin (*Lanes 1* and *4*), transgenic mouse skin (*Lanes 2* and *5*), or transgenic skin tumor (*Lanes 3* and *6*).

Table 1 *Comparison of tumor phenotype in K5 promoter-targeted Gli2ΔN2 and Gli2 transgenic mice*

| | *K5-Gli2ΔN2* | *K5-Gli2* |
|---|---|---|
| Tumor types | Multiple, few BCCs | BCCs |
| Location | Trunk > head > extremities ≫ tail | Tail > ears > head ≫ trunk |
| Growth rate | Variable | Slow |
| Phenotype first evident | 1–2 weeks | Usually after 3–4 weeks |
| Pigmented tumors | Minority | Nearly all |
| Tumorigenic cell lines | Yes | No |

**Development of Multiple Different Tumor Types in K5-Gli2ΔN2 Mice: Gross Appearance.** The gross phenotype of *K5-Gli2ΔN2* mice was distinct from that of *K5-Gli2* mice, with major differences, including (*a*) earlier development of visible skin abnormalities, (*b*) appearance of multiple tumor types, (*c*) highly variable tumor growth rates, and (*d*) predilection for different body sites (Table 1). Among the five founders who developed tumors, all exhibited a phenotype by 14 days after birth and developed multiple tumors between 3 weeks and 5 months of age. Two, founders 391 and 116, were runted and had substantially less hair than their littermates. By ~3 weeks of age, founder 391 had developed multiple tumors and expired at 4 weeks. Tumors were detected on founder 116 at ~4 weeks of age, and by 8 weeks almost the entire skin contained numerous tumors (Fig. 2*C*). The phenotypes of founders 426 and 427 were very similar: both showed linear regions completely devoid of hair by 1 week of age (Fig. 2*A*) and developed multiple rapidly growing tumors in these areas by 5–6 weeks of age. The fifth founder, founder 83, exhibited a small hairless area evident within the first week, but did not develop tumors until 5 months of age (Fig. 2*D*). In contrast to the early (within 1–2 weeks) initial appearance of skin abnormalities in *K5-Gli2ΔN2* mice, *K5-Gli2* mice rarely developed skin changes before 3–4 weeks of age.

Interestingly, tumors in *K5-Gli2ΔN2* mice frequently arose in locations different from those in *K5-Gli2* mice. Most of the tumors that developed in *K5-Gli2ΔN2* mice were located in dorsal skin overlying the trunk, with a few lesions on the head and limbs and two arising in footpads (Fig. 2*B*). No grossly visible tumors were detected in the skin on the ears of any of the *K5-Gli2ΔN2* transgenic founders, and only one founder developed lesions on the tail. In striking contrast, the tail, ears, and dorsal paws were sites at which the great majority of tumors arose in *K5-Gli2* mice (see Fig. 1 in Ref. 28), whereas grossly evident tumors were never observed in footpads of *K5-Gli2* mice. In addition, although BCCs arising in pigmented *K5-Gli2* mice were frequently dark brown or black because of melanin accumulation (see Fig. 1 in Ref. 28), this was uncommon in tumors arising in *K5-Gli2ΔN2* mice (Fig. 2). Finally, the growth rate of tumors in *K5-Gli2ΔN2* mice was highly variable. This was most apparent when comparing different tumors on the same animal as illustrated in Fig. 2, *E–H*. During a 10-day interval, there were no detectable changes in the sizes of tumors located on the limb (Fig. 2, *E* and *F*), whereas tumors on the side of the trunk enlarged dramatically during the same time interval (Fig. 2, *G* and *H*). In striking contrast, nearly all tumors arising in *K5-Gli2* mice had a similar gross appearance, and they all grew at a relatively slow rate, consistent with the behavior of BCCs in humans.

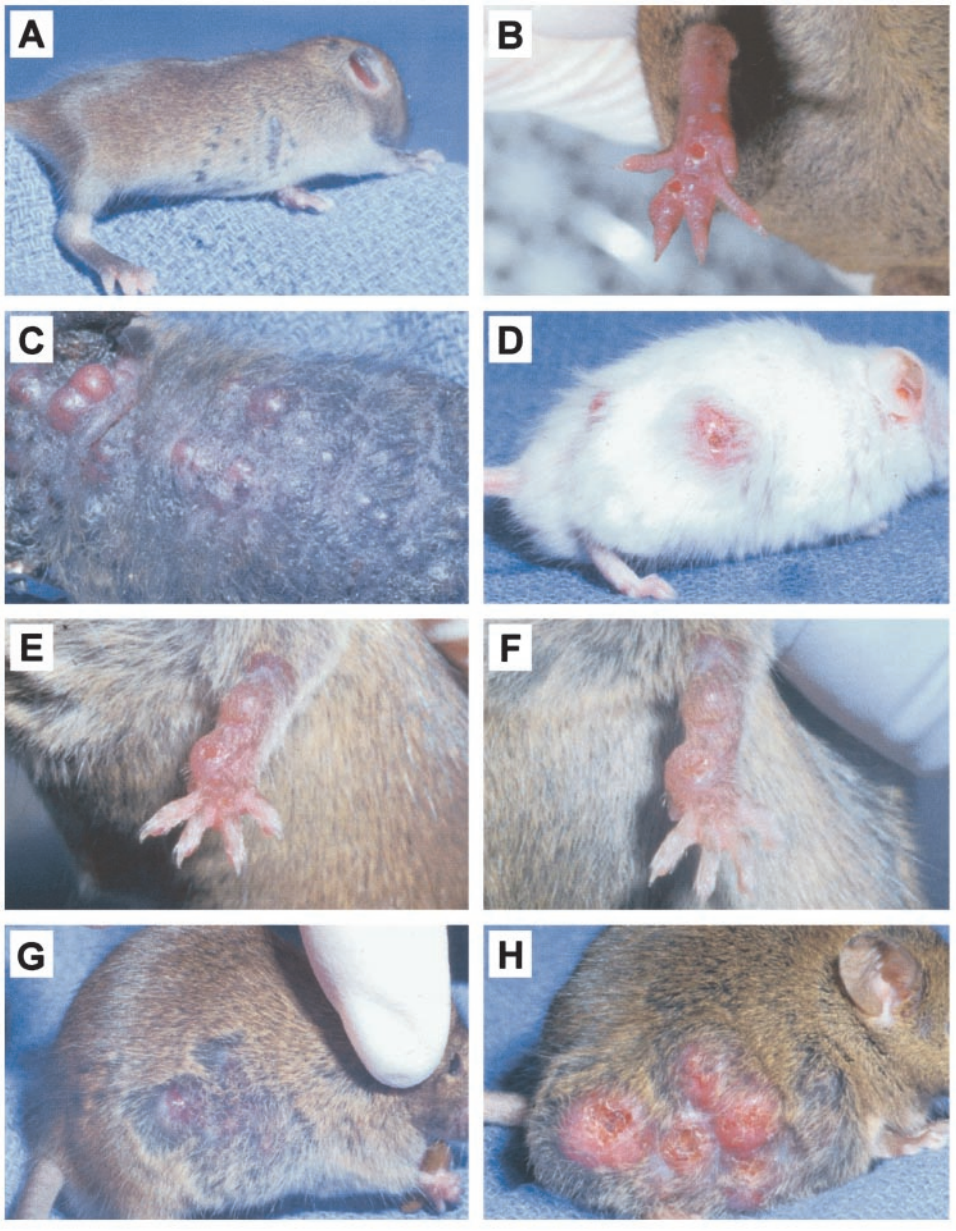


Fig. 2. Gross appearance and divergent growth rates of tumors arising in *K5-Gli2ΔN2* mice. *A* and *B*, founder 427 with hairless regions on dorsolateral skin at 10 days of age (*A*) and tumors arising in footpads at 8 weeks (*B*). Shown in *C* and *D* are numerous tumors throughout the skin of founder 116 at ~2 months of age (*C*) compared with small number of isolated lesions arising in founder 83 at ~6 months (*D*). *E–H*, divergent growth rates of different tumors in the same *K5-Gli2ΔN2* transgenic mouse (no. 427). The two sets of photographs were taken 10 days apart. Note the similar size of tumors on dorsum of paw (*E* and *F*) contrasted with dramatic increase in size of tumors on dorsolateral region (*G* and *H*) during the same interval.

**Histopathology and Marker Analysis.** The differences in behavior of individual tumors arising in *K5-Gli2ΔN2* mice suggested that they may be a less homogeneous population than the BCCs that developed in *K5-Gli2* mice. In fact, examination of H&E-stained sections revealed a multiplicity of tumor types in the skin of *K5-Gli2ΔN2* mice. The majority of tumors were histologically similar to human trichoblastomas, particularly the "rippled pattern" variant (39, 40). They contained numerous mitotic cells (Fig. 3*A*, *inset*), and large lesions had necrotic centers (*arrow* in Fig. 3*A*). A minority of tumor nodules contained pigment (*arrowheads* in Fig. 3*A*). Despite the massive size of many of these tumors, they did not invade surrounding tissues. A second tumor type appeared grossly similar to BCCs arising in *K5-Gli2* mice and grew at a similarly slow rate, but the histological features were consistent with a distinct tumor type called cylindroma (Fig. 3*B*). These lesions contain nests of basaloid cells closely approximating each other to resemble pieces of a jigsaw puzzle. The third type of lesion commonly seen in *K5-Gli2ΔN2* mice (Fig. 3*C*) was histologically similar to human basaloid follicular hamartoma (41). These lesions were composed of frond-like epithelial downgrowths with cellular nests and strands, resembling relatively undifferentiated hair follicle epithelium. To our surprise, only three BCCs (for example, see Fig. 3*D*) were identified in the five transgenic founders with tumors. Various other tumor types were observed (Fig. 3*E*) that were difficult to classify according to histological criteria used for identifying human skin tumors. These were generically classified as benign hair follicle tumors, with some exhibiting features of trichoadenoma or trichoepithelioma. *K5-Gli2ΔN2* mice also developed keratinized cysts within the dermis (Fig. 3*F*). It is notable that despite the large number and heterogeneity of tumors arising in *K5-Gli2ΔN2* mice, squamous neoplasms (papillomas, squamous cell carcinomas, or keratoacanthomas) were never observed.

The expression patterns of several protein markers support the concept that skin tumors arising in *K5-Gli2ΔN2* mice were derived from hair follicle epithelium, which is believed to contain progenitor cells for a variety of tumor types, including trichoblastomas and BCCs (42). Nearly all tumor cells in trichoblastomas contained K5 (Fig. 4*A*), which is usually detected in the basal layer of the epidermis and the outermost cell layers of the hair follicle (outer root sheath). K17,

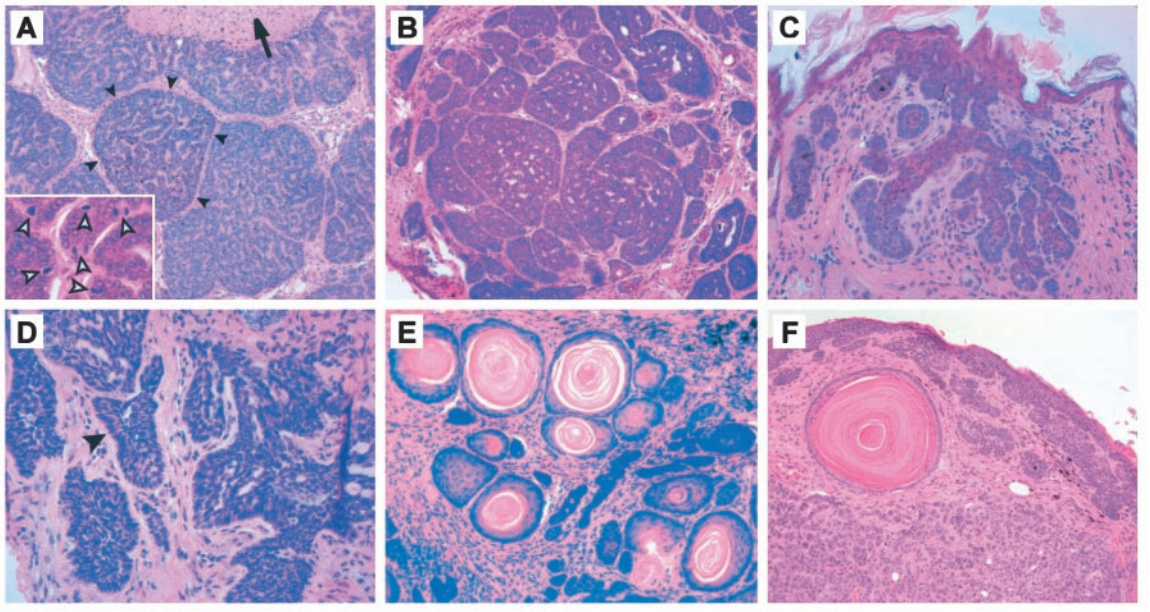


Fig. 3. Development of multiple distinct tumor phenotypes in *K5-Gli2ΔN2* mice, as shown by H&E staining. *A*, large tumor from founder 426, exhibiting cords or ribbons of basaloid cells with intervening eosinophilic material, resembling human rippled-pattern trichoblastomas. Large tumors commonly exhibited central necrosis (*arrow*) and frequent mitotic figures (*arrowheads* in *inset*). Note prominent accumulation of melanin in one of the tumor nodules, indicated by *black arrowheads*. *B*, tumor from founder 116, consisting of basaloid cells arranged as tightly fitting nests in a jigsaw-like pattern, similar to human cylindroma. *C*, basaloid follicular hamartoma from founder 427, with strands and nests of cells in a frond-like arrangement connected to the epidermis. *D*, tumor containing dense islands of homogeneous, basophilic cells, similar to human BCC. Note characteristic columnar arrangement of nuclei (palisading) at periphery of one of the tumor nests (*arrowhead*). *E*, benign follicular tumor arising in ear of founder 385, with features of trichoadenoma or trichoepithelioma. *F*, three distinct lesions in section from skin of founder 385, with basaloid follicular hamartoma-like lesion adjacent to the epidermis, keratinized cyst, and trichoblastoma occupying *lower portion* of section.

usually restricted to the outer root sheath and hair shaft precursor cells in normal adult skin (43, 44), was also detected in nearly all cells of trichoblastomas (Fig. 4*B*). Nearly all cells in other tumor types seen in *K5-Gli2ΔN2* mice were also immunoreactive for K5 and K17 (not shown). K6 is found in cells of the innermost (differentiating) layer of the outer root sheath (45) and in hyperplastic epidermis, and was detected in isolated cells or cell clusters within a subpopulation of tumor nests (not shown). Bcl-2, a useful diagnostic marker for human BCCs and trichoblastomas, was expressed diffusely throughout tumor nodules (Fig. 4*C*).

**Up-Regulation of *Gli2ΔN2* Transgene and Shh Target Genes in Tumors.** To assess whether there was a correlation between transgene expression levels, Shh pathway activity, and tumor phenotype, we isolated RNA from multiple tumors and skin for Northern blot analysis. In transgenic mouse skin without visible tumors, levels of *Gli2ΔN2* mRNA were minimal or undetectable (Fig. 5*A*, *Lane 9*). One sample from normal-appearing skin that contained microscopic tumors in adjacent tissue expressed a low level of *Gli2ΔN2* mRNA (Fig. 5*A*, *Lane 7*). All tumor samples contained substantial amounts of transgene mRNA, with large tumors generally expressing higher levels than relatively small tumors (Fig. 5*A*). Transgene expression in a single founder could thus vary from low or undetectable (in normal-appearing skin) to very high (in large tumors), revealing a strong association between transgene expression and tumorigenicity. Comparable results were obtained by immunoblotting, with much higher levels of Gli2ΔN2 protein detected in tumor samples than in normal-appearing skin (Fig. 1*D*). We examined the abundance of *Gli1* and *Ptch1* mRNA to assess the level of Shh pathway activation and found a strong correlation with transgene expression levels (Fig. 5*A*). These findings are consistent with the concept that differences in the level of Shh pathway activity in *K5-Gli2ΔN2* mice can lead to distinct tumor phenotypes in skin. Given the dramatically increased transcriptional activity of Gli2ΔN2 compared with Gli2 in cultured cells, additional RNA analysis was performed using TaqMan PCR to quantify Shh target gene expression in control skin and tumors derived from *K5-Gli2ΔN2* and *K5-Gli2* mice. Although *Gli1*, *Ptch1*, and *Ptch2* mRNA all appeared higher in *K5-Gli2ΔN2* tumors than those from *K5-Gli2* mice, only *Gli1* expression was significantly elevated, and the increase was $<$2-fold (Fig. 5*B*). These data suggest that the distinct tumor phenotypes in *K5-Gli2* and *K5-Gli2ΔN2* transgenic mice are

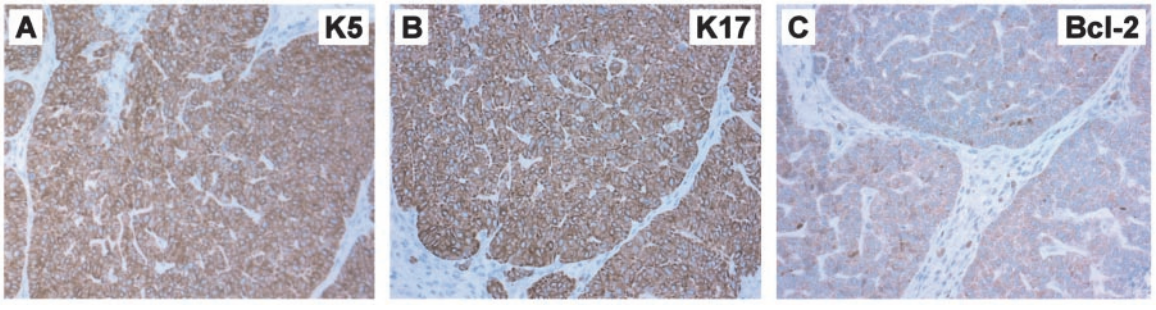


Fig. 4. Protein marker expression in trichoblastomas arising in *K5-Gli2ΔN2* mice. K5 (*A*) and K17 (*B*), expressed in the outer root sheath of hair follicles and many follicle-derived tumors, are detected in essentially all tumor cells. Bcl-2, a marker for human BCCs and trichoblastomas, is expressed in mouse trichoblastomas (*C*).

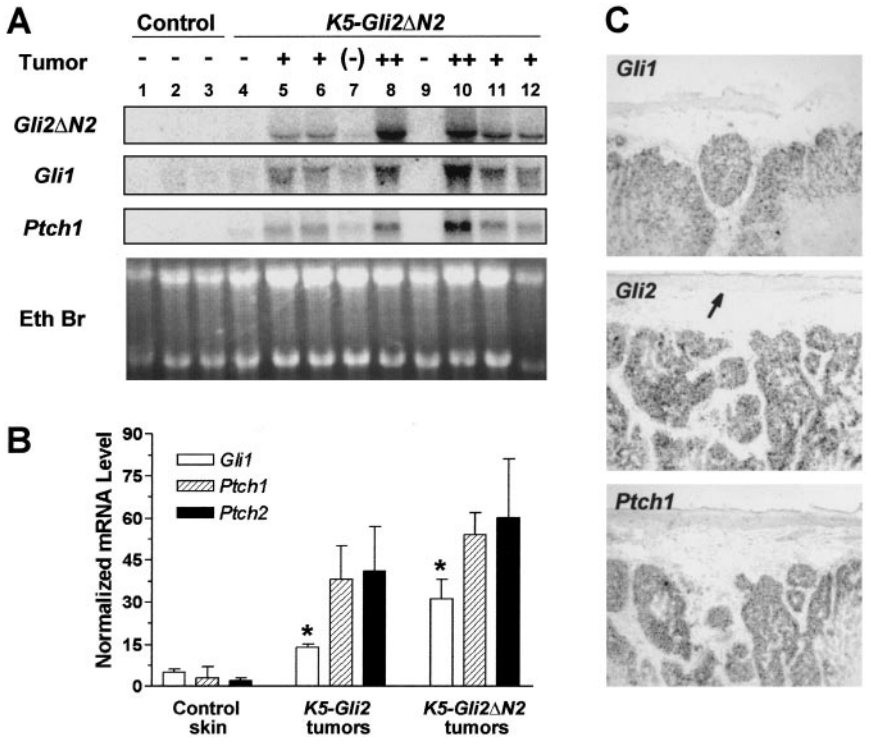


Fig. 5. Expression of *Gli2ΔN2* mRNA and Shh target genes in skin tumors. *A*, total RNA was isolated from skin of control mice (*Lanes 1–3*) and transgenic mice with no detectable phenotype (*Lanes 4* and *9*); microscopic tumor, detected in adjacent skin (*Lane 7*); small tumors (*Lanes 5*, *6*, *11*, and *12*); or large tumors (*Lanes 8* and *10*). $^{32}$P-labeled probes were used to quantify the abundance of indicated transcripts, and ethidium bromide (*Eth Br*) staining of the agarose gel was used as a measure of total RNA loading. *B*, TaqMan analysis comparing Shh target gene expression in control mouse skin ($n = 3$), *K5-Gli2* tumors ($n = 4$), and *K5-Gli2ΔN2* tumors ($n = 5$; same samples as in *Lanes 5*, *6*, *8*, *10*, and *11* in *panel A*). Although *Gli1*, *Ptch1*, and *Ptch2* levels appeared higher in *K5-Gli2ΔN2* tumors than in *K5-Gli2* tumors, only *Gli1* was significantly elevated ($P < 0.01$, Student's *t* test). Comparable levels of *Gli2/Gli2ΔN2* mRNA, representing endogenous and transgenic mRNA, were detected in the *K5-Gli2* and *K5-Gli2ΔN2* tumor samples (not shown). *C*, *in situ* hybridization revealing localization of *Gli2/Gli2ΔN2* and Shh target gene mRNA specifically in tumor cells. Note that transgene expression levels are not detectably elevated in overlying epidermis (*arrow* in *middle panel*).

not likely attributable to differences in the overall level of Shh pathway activation. *In situ* analysis revealed that *Gli2/Gli2ΔN2* mRNA, as well as *Gli1* and *Ptch1* mRNA, was expressed specifically in tumor epithelium (Fig. 5*C*).

**Establishment of Tumorigenic Cell Lines from K5-Gli2ΔN2 Tumors.** In contrast to many other epithelial malignancies, human BCCs grow slowly and rarely metastasize (reviewed in Ref. 46). The indolent nature of these tumors is associated with an inability to establish BCC cell lines that retain their tumorigenicity in nude mouse xenografts; this has been a major impediment to progress in the field. The rapid growth of many tumors arising in *K5-Gli2ΔN2* mice prompted our attempts to generate cell lines from several of these lesions. We established a total of 10 cell lines from four different tumors. Analysis of the first two cell lines that were established revealed continued *Gli2ΔN2* mRNA and protein expression (Fig. 6). Moreover, the Shh pathway was constitutively activated in these cells *in vitro*, based on up-regulation of *Gli1* and *Ptch1* mRNA (Fig. 6). These cell lines were highly tumorigenic when injected s.c. into nude

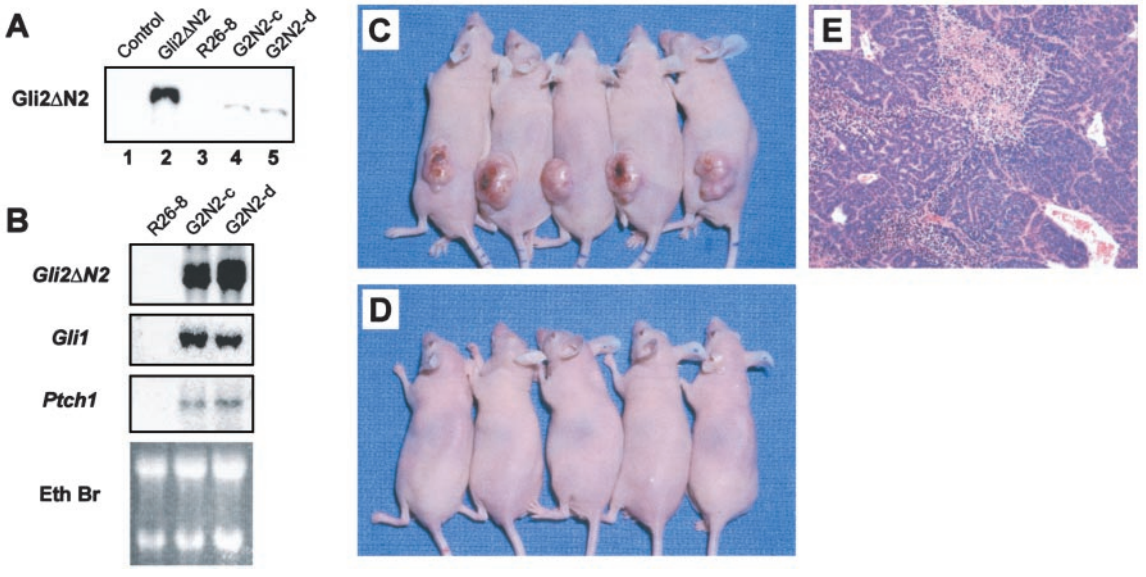


Fig. 6. Characterization of cell lines derived from a trichoblastoma arising in a *K5-Gli2ΔN2* transgenic mouse. *A*, protein lysates were obtained from an SV40-transformed human keratinocyte cell line transiently transfected with either pcDNA3.1 plasmid (*Control*) or pcDNA3.1HisBGli2ΔN2 (*Gli2ΔN2*). Lysates were also prepared from a control mouse keratinocyte cell line (*R26-8*) and two cell lines, (G2N2-c, G2N2-d), derived from a trichoblastoma arising in a *K5-Gli2ΔN2* transgenic mouse. Samples were immunoprecipitated and blotted using polyclonal anti-His antibody. *B*, Northern blot analysis of RNA from indicated cell lines. Note expression of *Gli2ΔN2* transgene and up-regulation of Shh target genes *Gli1* and *Ptch1*, indicating constitutive activation of Shh signaling in tumor cell lines *in vitro*. *C*, tumor development in nude mice 25 days after s.c. injection of the G2N2c cell line. Similar results were seen with the G2N2d cell line (not shown). *D*, control mouse keratinocyte cell line R26-8 does not produce tumors after s.c. injection. *E*, histology of nude mouse tumors resembles that seen in trichoblastomas arising in founders (see Fig. 3*A*).

mice, with tumors first evident 7–10 days after injection. The rapid growth rate and histology were similar to those of the original tumor, a trichoblastoma, from which these lines were generated (compare Figs. 6*E* and 3*A*). These findings strongly suggest that mouse trichoblastomas are biologically distinct from BCCs and further strengthen the concept that the oncogenic potential of *Gli2*Δ*N2* differs from that of *Gli2*.

## DISCUSSION

The consistent up-regulation of Shh target genes in nearly all human BCCs examined suggests a central role for Shh transcriptional effectors in tumorigenesis. In keeping with this hypothesis, skin-targeted overexpression of *Gli2* or *GLI1* by use of a *K5* promoter is sufficient to produce BCCs in transgenic mice, although *K5-GLI1* mice preferentially developed other types of skin tumors. In this report, we have mimicked the *K5-GLI1* tumor phenotype by skin-targeted overexpression of a *Gli2* mutant, *Gli2*Δ*N2*. Our findings reveal a previously unsuspected role for the $NH_2$-terminal domain of Gli2 in defining skin tumor phenotype.

Several transgenic models have been generated to examine the involvement of deregulated Shh signaling in cutaneous tumorigenesis. Skin-targeted overexpression of *SHH* by use of a *K14* promoter (47), or the gain-of-function *M2SMO* mutant by use of a *K5* promoter (48), resulted in development of basaloid proliferations in skin of late-stage embryos or newborn mice. *Ptch1*$^{lacZ/+}$ mutant mice develop visible skin tumors 6–9 months after exposure to ionizing or UV radiation (49); both of these agents also enhance human BCC development. The tumor phenotype of *K5-GLI1* mice reported by Nilsson *et al.* (29) is particularly interesting in light of our studies with *Gli2* and the *Gli2*Δ*N2* mutant. *K5-GLI1* transgenics develop several types of skin tumors, including trichoblastomas, cylindromas, trichoepitheliomas, and BCCs (29), whereas *K5-Gli2* mice develop only BCCs (28). These divergent tumor spectra suggest that *Gli2* and *GLI1* are not equivalent in terms of their oncogenic potential, which is in keeping with results of studies exploring the function of these molecules in mouse embryogenesis (10).

The qualitative difference in tumorigenicity of Gli2 and Gli2ΔN2 in skin was unexpected. Given the increased *in vitro* transcriptional activity of Gli2ΔN2 and its ability (unlike full-length Gli2) to activate Shh target genes in the dorsal neural tube *in vivo* (30), we anticipated that Gli2ΔN2 would be substantially more potent than Gli2 at activating Shh signaling in skin. However, comparison of Shh target gene expression in tumors from *K5-Gli2*Δ*N2* and *K5-Gli2* mice failed to reveal significant differences with the notable exception of *Gli1*, which was approximately twice as abundant in *K5-Gli2*Δ*N2* tumors (Fig. 5*B*). These findings underscore the importance of cellular context when examining responses to Gli proteins and raise the interesting possibility that the multiplicity of tumor types in *K5-Gli2*Δ*N2* mice is indirectly attributable to modestly enhanced expression of endogenous *Gli1*. This could also be partly responsible for the greater potency of *Gli2*Δ*N2* in reporter assays (Fig. 1 and Ref. 30) that do not distinguish between exogenous and endogenous Gli molecules. In keeping with this hypothesis, the mouse *Gli1* promoter contains several Gli binding sites and has been shown to be activated by Gli3 (50); it would presumably be activated by Gli2 and Gli2ΔN2 as well.

An alternative explanation for our findings would attribute differences in tumor phenotype to qualitative differences in the oncogenic potential of Gli2ΔN2 and full-length Gli2 that are independent of effects on Gli transcriptional activity. This possibility implies an important regulatory function for the Gli2 $NH_2$ terminus that may involve direct interaction with other signaling molecules, and its presence in *K5-Gli2* mice may either promote BCC development or repress formation of other follicle-derived tumor types seen in *K5-Gli2*Δ*N2* and *K5-GLI1* mice. Support for, or against, this hypothesis could be obtained by assessing the phenotype of *K5* promoter-driven transgenic mice expressing a Gli2-GLI1 chimera containing the Gli2 $NH_2$-terminal fragment that is deleted in Gli2ΔN2.

In addition to the disparate tumor phenotypes in *K5-Gli2* and *K5-Gli2*Δ*N2* mice, there are several other distinctions (Table 1). One of the most striking is the predisposition of tumors in *K5-Gli2* mice to arise in certain locations on the body, including the tail, ears, and dorsal paws. This finding suggests strong regional differences in the susceptibility of skin to form tumors in response to *K5* promoter-driven *Gli2*, but not *Gli2*Δ*N2* or *GLI1*. Whether this is related to differences in transgene expression levels or reflects an intrinsic difference in responsiveness of keratinocytes residing in these regions is not known. The increased occurrence of human BCCs in certain locations is frequently attributed to the mutagenic effects of increased sun exposure, but regional differences in susceptibility to human BCC development may also exist.

The focal appearance of tumors in *K5-Gli2*Δ*N2* and *K5-Gli2* mice is also notable given the fact that the *K5* promoter is active throughout the epidermal basal layer and outer root sheath of hair follicles (27, 51). Focal tumor development is not restricted to *K5-Gli2* founders and thus is unlikely to be the result of mosaicism. Because transgene expression can exhibit substantial cell-to-cell variability in the same animal (52–55), we propose that focal tumors reflect outgrowth of a relatively small number of cells with the sufficiently high transgene expression levels needed to drive tumorigenesis. This concept is supported by our (*a*) Northern data, in which *Gli2*Δ*N2* transgene expression was markedly higher in all tumor samples than in unaffected transgenic skin (Fig. 5*A*); (*b*) *in situ* analysis, where only tumor cells were found to express high levels of transgene mRNA (Fig. 5*C*); and (*c*) immunoblot analysis (Fig. 1). Similarly, *Gli2* mRNA was readily detected in BCCs arising in *K5-Gli2* mice, whereas expression of *Gli2* in the adjacent epidermal basal layer was below the level of detection (Fig. 2E in Ref. 28). Although sufficiently high expression of positive-acting Gli transcription factors is likely to play a central role in the genesis of certain follicle-derived skin tumors, the downstream target genes driving this process and how they alter keratinocyte biology are not yet known.

Despite the appearance of multiple tumor types in *K5-Gli2*Δ*N2* mice, none of them resembled squamous neoplasms, which are common in other transgenic models overexpressing a variety of growth factors, receptor tyrosine kinases, or oncogenes in skin (reviewed in Refs. 56–58). Cutaneous squamous cell carcinomas, like other epithelial malignancies, develop through a series of morphological stages that are accompanied by multiple genetic alterations (59, 60). In contrast, BCC precursor lesions have not been identified, and there is no evidence of neoplastic progression in this tumor type. Constitutive Shh signaling is detected even in microscopic human BCCs and, based on several mouse models, may be sufficient for the development and maintenance of these tumors. Mechanism-based approaches to BCC treatment and/or prevention may thus require only effective inhibition of the Shh pathway.

The development of multiple tumor types in *K5-Gli2*Δ*N2* mice strengthens the notion that deregulation of Shh signaling can give rise to a variety of appendage-derived tumors in skin (reviewed in Ref. 61), but the basis for tumor heterogeneity in this mouse model is not known. One possibility is that different levels of Shh pathway activity, even in the same progenitor cell, will yield different tumors. A similar proposal was put forth to explain tumor heterogeneity in *K5-GLI1* mice (29). Although the Northern results presented in Fig. 5*A* are consistent with this interpretation, direct support for this hypothesis awaits the development of an inducible mouse model in which *Gli*

transgene expression can be maintained at different levels and the resultant tumor phenotypes evaluated. Another possibility is that spontaneous mutations are occurring in initially homogeneous *K5-Gli2ΔN2* tumors, driving the outgrowth of some cells into histologically distinct tumor phenotypes. Although this possibility cannot formally be excluded, the simultaneous appearance of multiple tumor types in young mice argues against it. In addition, at least in the case of BCCs, tumor phenotype in both humans and *K5-Gli2* mice is remarkably stable. Finally, the different tumors arising in *K5-Gli2ΔN2* mice may result from expansion of progenitor cells at different stages of hair follicle maturation. This hypothesis can be tested by overexpressing *Gli2ΔN2* in cutaneous keratinocytes by use of promoters with a more restricted expression pattern than *K5*, a strategy previously used with the v-$ras^{Ha}$ oncogene to probe the relationship between target cell and tumor type (62).

## ACKNOWLEDGMENTS

We are grateful to Drs. Jose Jorcano, Pierre Coulombe, and Richard Schlegel for providing reagents. We appreciate Ted Hamilton's assistance with statistical analysis, George Cotsarelis' comments on the manuscript, and production of transgenic mice by members of the University of Michigan Transgenic Core.

## REFERENCES

1. Chuang, P. T., and Kornberg, T. B. On the range of hedgehog signaling. Curr. Opin. Genet. Dev., *10:* 515–522, 2000.
2. Ingham, P. W., and McMahon, A. P. Hedgehog signaling in animal development: paradigms and principles. Genes Dev., *15:* 3059–3087, 2001.
3. Kalderon, D. Transducing the hedgehog signal. Cell, *103:* 371–374, 2000.
4. Aza-Blanc, P., and Kornberg, T. B. Ci: a complex transducer of the hedgehog signal. Trends Genet., *15:* 458–462, 1999.
5. Matise, M. P., and Joyner, A. L. Gli genes in development and cancer. Oncogene, *18:* 7852–7859, 1999.
6. Altaba, A. Gli proteins and Hedgehog signaling: development and cancer. Trends Genet., *15:* 418–425, 1999.
7. Hynes, M., Stone, D. M., Dowd, M., Pitts-Meek, S., Goddard, A., Gurney, A., and Rosenthal, A. Control of cell pattern in the neural tube by the zinc finger transcription factor and oncogene Gli-1. Neuron, *19:* 15–26, 1997.
8. Lee, J., Platt, K. A., Censullo, P., and Ruiz i Altaba. A. Gli1 is a target of Sonic hedgehog that induces ventral neural tube development. Development, *124:* 2537–2552, 1997.
9. Altaba, A. Combinatorial Gli gene function in floor plate and neuronal inductions by Sonic hedgehog. Development, *125:* 2203–2212, 1998.
10. Park, H. L., Bai, C., Platt, K. A., Matise, M. P., Beeghly, A., Hui, C. C., Nakashima, M., and Joyner, A. L. Mouse Gli1 mutants are viable but have defects in SHH signaling in combination with a Gli2 mutation. Development, *127:* 1593–1605, 2000.
11. Mo, R., Freer, A. M., Zinyk, D. L., Crackower, M. A., Michaud, J., Heng, H. H., Chik, K. W., Shi, X. M., Tsui, L. C., Cheng, S. H., Joyner, A. L., and Hui, C. Specific and redundant functions of Gli2 and Gli3 zinc finger genes in skeletal patterning and development. Development, *124:* 113–123, 1997.
12. Motoyama, J., Liu, J., Mo, R., Ding, Q., Post, M., and Hui, C. C. Essential function of Gli2 and Gli3 in the formation of lung, trachea and oesophagus. Nat. Genet., *20:* 54–57, 1998.
13. Hardcastle, Z., Mo, R., Hui, C. C., and Sharpe, P. T. The Shh signalling pathway in tooth development: defects in Gli2 and Gli3 mutants. Development, *125:* 2803–2811, 1998.
14. Matise, M. P., Epstein, D. J., Park, H. L., Platt, K. A., and Joyner, A. L. Gli2 is required for induction of floor plate and adjacent cells, but not most ventral neurons in the mouse central nervous system. Development, *125:* 2759–2770, 1998.
15. Ding, Q., Motoyama, J., Gasca, S., Mo, R., Sasaki, H., Rossant, J., and Hui, C. C. Diminished Sonic hedgehog signaling and lack of floor plate differentiation in Gli2 mutant mice. Development, *125:* 2533–2543, 1998.
16. St. Jacques, B., Dassule, H. R., Karavanova, I., Botchkarev, V. A., Li, J., Danielian, P. S., McMahon, J. A., Lewis, P. M., Paus, R., and McMahon, A. P. Sonic hedgehog signaling is essential for hair development. Curr. Biol., *8:* 1058–1068, 1998.
17. Chiang, C., Swan, R. Z., Grachtchouk, M., Bolinger, M., Litingtung, Y., Robertson, E. K., Cooper, M. K., Gaffield, W., Westphal, H., Beachy, P. A., and Dlugosz, A. A. Essential role for sonic hedgehog during hair follicle morphogenesis. Dev. Biol., *205:* 1–9, 1999.
18. Karlsson, L., Bondjers, C., and Betsholtz, C. Roles for PDGF-A and sonic hedgehog in development of mesenchymal components of the hair follicle. Development, *126:* 2611–2621, 1999.
19. Gorlin, R. J. Nevoid basal-cell carcinoma syndrome. Medicine, *66:* 98–113, 1987.
20. Johnson, R. L., Rothman, A. L., Xie, J., Goodrich, L. V., Bare, J. W., Bonifas, J. M., Quinn, A. G., Myers, R. M., Cox, D. R., Epstein, E. H., Jr., and Scott. M. P. Human homolog of patched, a candidate gene for the basal cell nevus syndrome. Science (Wash. DC), *272:* 1668–1671, 1996.
21. Hahn, H., Wicking, C., Zaphiropoulos, P. G., Gailani, M. R., Shanley, S., Chidambaram, A., Vorechovsky, I., Holmberg, E., Unden, A. B., Gillies, S., Negus, K., Smyth, I., Pressman, C., Leffell, D. J., Gerrard, B., Goldstein, A. M., Dean, M., Toftgard, R., Chenevix-Trench, G., Wainwright, B., and Bale, A. E. Mutations of the human homolog of *Drosophila* patched in the nevoid basal cell carcinoma syndrome. Cell, *85:* 841–851, 1996.
22. Gailani, M. R., Stahle-Backdahl, M., Leffell, D. J., Glynn, M., Zaphiropoulos, P. G., Pressman, C., Unden, A. B., Dean, M., Brash, D. E., Bale, A. E., and Toftgard, R. The role of the human homologue of *Drosophila* patched in sporadic basal cell carcinomas. Nat. Genet., *14:* 78–81, 1996.
23. Wolter, M., Reifenberger, J., Sommer, C., Ruzicka, T., and Reifenberger, G. Mutations in the human homologue of the *Drosophila* segment polarity gene patched (PTCH) in sporadic basal cell carcinomas of the skin and primitive neuroectodermal tumors of the central nervous system. Cancer Res., *57:* 2581–2585, 1997.
24. Aszterbaum, M., Rothman, A., Johnson, R. L., Fisher, M., Xie, J., Bonifas, J. M., Zhang, X., Scott, M. P., and Epstein, E. H. J. Identification of mutations in the human PATCHED gene in sporadic basal cell carcinomas and in patients with the basal cell nevus syndrome. J. Investig. Dermatol., *110:* 885–888, 1998.
25. Dahmane, N., Lee, J., Robins, P., Heller, P., and Ruiz i Altaba, A. Activation of the transcription factor Gli1 and the sonic hedgehog signalling pathway in skin tumours. Nature (Lond.), *389:* 876–881, 1997.
26. Unden, A. B., Zaphiropoulos, P. G., Bruce, K., Toftgard, R., and Stahle-Backdahl, M. Human patched (PTCH) mRNA is overexpressed consistently in tumor cells of both familial and sporadic basal cell carcinoma. Cancer Res., *57:* 2336–2340, 1997.
27. Ramirez, A., Bravo, A., Jorcano, J. L., and Vidal, M. Sequences 5′ of the bovine keratin 5 gene direct tissue- and cell-type-specific expression of a lacZ gene in the adult and during development. Differentiation, *58:* 53–64, 1994.
28. Grachtchouk, M., Mo, R., Yu, S., Zhang, X., Sasaki, H., Hui, C. C., and Dlugosz, A. A. Basal cell carcinomas in mice overexpressing Gli2 in skin. Nat. Genet., *24:* 216–217, 2000.
29. Nilsson, M., Unden, A. B., Krause, D., Malmqwist, U., Raza, K., Zaphiropoulos, P. G., and Toftgard, R. Induction of basal cell carcinomas and trichoepitheliomas in mice overexpressing GLI-1. Proc. Natl. Acad. Sci. USA, *97:* 3438–3443, 2000.
30. Sasaki, H., Nishizaki, Y., Hui, C., Nakafuku, M., and Kondoh, H. Regulation of Gli2 and Gli3 activities by an amino-terminal repression domain: implication of Gli2 and Gli3 as primary mediators of Shh signaling. Development, *126:* 3915–3924, 1999.
31. Pietenpol, J. A., Stein, R. W., Moran, E., Yaciuk, P., Schlegel, R., Lyons, R. M., Pittelkow, M. R., Münger, K., Howley, P. M., and Moses, H. L. TGF-β1 inhibition of c-*myc* transcription and growth in keratinocytes is abrogated by viral transforming proteins with pRB binding domains. Cell, *61:* 777–785, 1990.
32. Sasaki, H., Hui, C., Nakafuku, M., and Kondoh, H. A binding site for Gli proteins is essential for HNF-3β floor plate enhancer activity in transgenics and can respond to Shh *in vitro*. Development, *124:* 1313–1322, 1997.
33. Brasier, A. R., Tate, J. E., and Habener, J. F. Optimized use of the firefly luciferase assay as a reporter gene in mammalian cell lines. Biotechniques, *7:* 1116–1122, 1989.
34. Hui, C. C., and Joyner, A. L. A mouse model of greig cephalopolysyndactyly syndrome: the extra-toesJ mutation contains an intragenic deletion of the Gli3 gene. Nat. Genet., *3:* 241–246, 1993.
35. Dlugosz, A. A., Glick, A. B., Tennenbaum, T., Weinberg, W. C., and Yuspa, S. H. Isolation and utilization of epidermal keratinocytes for oncogene research. Methods Enzymol., *254:* 3–20, 1995.
36. Zambrowicz, B. P., Imamoto, A., Fiering, S., Herzenberg, L. A., Kerr, W. G., and Soriano, P. Disruption of overlapping transcripts in the ROSA β geo 26 gene trap strain leads to widespread expression of beta-galactosidase in mouse embryos and hematopoietic cells. Proc. Natl. Acad. Sci. USA, *94:* 3789–3794, 1997.
37. Cotsarelis, G., Sun, T. T., and Lavker, R. M. Label-retaining cells reside in the bulge area of pilosebaceous unit: implications for follicular stem cells, hair cycle, and skin carcinogenesis. Cell, *61:* 1329–1337, 1990.
38. Lavker, R. M., Miller, S., Wilson, C., Cotsarelis, G., Wei, Z. G., Yang, J. S., and Sun, T. T. Hair follicle stem cells: their location, role in hair cycle, and involvement in skin tumor formation. J. Investig. Dermatol., *101*: 16S–26S, 1993.
39. Yamamoto, O., Hisaoka, M., Yasuda, H., Nishio, D., and Asahi, M. A rippled-pattern trichoblastoma: an immunohistochemical study. J. Cutan. Pathol., *27:* 460–465, 2000.
40. Akasaka, T., Imamura, Y., Mori, Y., Iwasaki, M., and Kon, S. Trichoblastoma with rippled-pattern. J. Dermatol., *24:* 174–178, 1997.
41. Nelson, B. R., Johnson, T. M., Waldinger, T., Gillard, M., and Lowe, L. Basaloid follicular hamartoma: a histologic diagnosis with diverse clinical presentations. Arch. Dermatol., *129:* 915–917, 1993.
42. Schirren, C. G., Rutten, A., Kaudewitz, P., Diaz, C., McClain, S., and Burgdorf, W. H. Trichoblastoma and basal cell carcinoma are neoplasms with follicular differentiation sharing the same profile of cytokeratin intermediate filaments. Am. J. Dermatopathol., *19:* 341–350, 1997.
43. McGowan, K. M., and Coulombe, P. A. Expression of keratin 17 coincides with the definition of major epithelial lineages during skin development. J. Cell. Biol., *143:* 469–486, 1998.
44. Panteleyev, A. A., Paus, R., Wanner, R., Nurnberg, W., Eichmuller, S., Thiel, R., Zhang, J., Henz, B. M., and Rosenbach, T. Keratin 17 gene expression during the murine hair cycle. J. Investig Dermatol., *108:* 324–329, 1997.
45. Rothnagel, J. A., and Roop, D. R. Hair follicle companion layer: reacquainting an old friend. J. Investig, Dermatol., *104*: 42S–43S, 1995.
46. Miller, S. J. Etiology and pathogenesis of basal cell carcinoma. Clin. Dermatol., *13:* 527–536, 1995.

47. Oro, A. E., Higgins, K. M., Hu, Z. L., Bonifas, J. M., Epstein, E. H., Jr., and Scott, M. P. Basal cell carcinomas in mice overexpressing sonic hedgehog. Science (Wash. DC), *276:* 817–821, 1997.
48. Xie, J., Murone, M., Luoh, S. M., Ryan, A., Gu, Q., Zhang, C., Bonifas, J. M., Lam, C. W., Hynes, M., Goddard, A., Rosenthal, A., Epstein, E. H. J., and de Sauvage, F. Activating Smoothened mutations in sporadic basal-cell carcinoma. Nature (Lond.), *391:* 90–92, 1998.
49. Aszterbaum, M., Epstein, J., Oro, A., Douglas, V., LeBoit, P. E., Scott, M. P., and Epstein, E. H., Jr. Ultraviolet and ionizing radiation enhance the growth of BCCs and trichoblastomas in patched heterozygous knockout mice. Nat. Med., *5:* 1285–1291, 1999.
50. Dai, P., Akimaru, H., Tanaka, Y., Maekawa, T., Nakafuku, M., and Ishii, S. Sonic Hedgehog-induced activation of the Gli1 promoter is mediated by GLI3. J. Biol. Chem., *274:* 8143–8152, 1999.
51. Byrne, C., Tainsky, M., and Fuchs, E. Programming gene expression in developing epidermis. Development, *120:* 2369–2383, 1994.
52. Ramirez, A., Milot, E., Ponsa, I., Marcos-Gutierrez, C., Page, A., Santos, M., Jorcano, J., and Vidal, M. Sequence and chromosomal context effects on variegated expression of keratin 5/lacz constructs in stratified epithelia of transgenic mice. Genetics, *158:* 341–350, 2001.
53. Dobie, K. W., Lee, M., Fantes, J. A., Graham, E., Clark, A. J., Springbett, A., Lathe, R., and McClenaghan, M. Variegated transgene expression in mouse mammary gland is determined by the transgene integration locus. Proc. Natl. Acad. Sci. USA, *93:* 6659–6664, 1996.
54. Porter, S. D., and Meyer, C. J. A distal tyrosinase upstream element stimulates gene expression in neural-crest-derived melanocytes of transgenic mice: position-independent and mosaic expression. Development, *120:* 2103–2111, 1994.
55. Morley, S. D., Viard, I., Chung, B. C., Ikeda, Y., Parker, K. L., and Mullins, J. J. Variegated expression of a mouse steroid 21-hydroxylase/$\beta$-galactosidase transgene suggests centripetal migration of adrenocortical cells. Mol. Endocrinol., *10:* 585–598, 1996.
56. Greenhalgh, D. A., and Roop, D. R. Dissecting molecular carcinogenesis: development of transgenic mouse models by epidermal gene targeting. Adv. Cancer Res., *64:* 247–296, 1994.
57. Arbeit, J. M. Transgenic models of epidermal neoplasia and multistage carcinogenesis. Cancer Surv., *26:* 7–34, 1996.
58. Brown, K., Burns, P. A., and Balmain, A. Transgenic approaches to understanding the mechanisms of chemical carcinogenesis in mouse skin. Toxicol. Lett., *82–83*: 123–130, 1995.
59. Yuspa, S. H. The pathogenesis of squamous cell cancer: lessons learned from studies of skin carcinogenesis—Thirty-third G. H. A. Clowes Memorial Award lecture. Cancer Res., *54:* 1178–1189, 1994.
60. Frame, S., Crombie, R., Liddell, J., Stuart, D., Linardopoulos, S., Nagase, H., Portella, G., Brown, K., Street, A., Akhurst, R., and Balmain, A. Epithelial carcinogenesis in the mouse: correlating the genetics and the biology. Philos. Trans. R. Soc. Lond. B Biol. Sci., *353:* 839–845, 1998.
61. Callahan, C. A., and Oro, A. E. Monstrous attempts at adnexogenesis: regulating hair follicle progenitors through Sonic hedgehog signaling. Curr. Opin. Genet. Dev., *11:* 541–546, 2001.
62. Brown, K., Strathdee, D., Bryson, S., Lambie, W., and Balmain, A. The malignant capacity of skin tumours induced by expression of a mutant H-ras transgene depends on the cell type targeted. Curr. Biol., *8:* 516–524, 1998.